

Analysis of the moving photocarrier grating technique for semiconductors of high defect density

J. A. Schmidt

INTEC (UNL-CONICET), Güemes 3450, 3000 Santa Fe, Argentina

M. Hundhausen and L. Ley

Institut für Technische Physik, Universität Erlangen-Nürnberg, Erwin-Rommel-Str. 1, D-91058 Erlangen, Germany

(Received 28 February 2001; published 2 August 2001)

The moving photocarrier grating (MPG) technique allows us to determine the carrier drift mobilities and the recombination lifetime of semiconductors. This technique utilizes a spatially and temporally modulated light intensity for the generation of photocarriers, which leads to a modulation of the carrier densities. The different mobilities of electrons and holes introduce a phase shift between the charge distributions. The resulting internal electric field produces a short circuit current which depends on the modulation frequency. The theoretical calculation of that short circuit current includes the diffusion and drift currents, and the generation and recombination processes. In the original treatment of the MPG method recombination between electrons and holes was assumed to proceed only through band-to-band transitions. We analyze here the MPG method by explicitly considering recombination through dangling bond states. We simulate short circuit current curves and compare them with measurements. The inclusion of recombination through dangling bonds allows us to explain an apparent contradiction in the evolution of the recombination lifetime as a function of light-induced degradation.

DOI: 10.1103/PhysRevB.64.104201

PACS number(s): 73.50.Gr, 73.50.Pz, 72.20.Jv, 72.40.+w

I. INTRODUCTION

The moving photocarrier grating (MPG) technique was presented in 1993 by Haken, Hundhausen, and Ley¹ (HHL) as a method to measure the drift mobility of electrons and holes (μ_n, μ_p) and the recombination lifetime (τ_R) of semiconductors. The method has been successfully applied to measure the transport parameters of *a*-Si:H and related materials.²⁻⁵ In the original treatment of HHL, recombination between electrons and holes is assumed to proceed only through band-to-band transitions. However, in amorphous semiconductors recombination is known to proceed mainly through dangling bond states. Upon prolonged illumination the defect density of hydrogenated amorphous silicon increases by orders of magnitude, a phenomenon which is known as the Staebler-Wronski effect.⁶ Under these circumstances, an analysis of the MPG technique including the complete recombination processes is required. By using conventional techniques it is difficult to study the changes in drift mobility and recombination lifetime upon illumination separately. Hence, most of the light-soaking studies have dealt with the decay of the photoconductivity up to now. Therefore, a complete analysis of the MPG method—including recombination through dangling bond states—could provide useful additional information in order to clarify experiments of light-induced degradation.

In this paper we perform MPG measurements as a function of illumination time to follow the light-induced degradation of hydrogenated amorphous silicon (*a*-Si:H). A fit of the MPG curves according to the formula deduced by HHL in Ref. 2 gives as a result an apparent increase of the recombination lifetime with the illumination time, in contrast to the well-known increase of the defect density. However, a more complete analysis of the MPG method, including

recombination through dangling bond states, allows us to clarify this point.

II. EXPERIMENT

The *a*-Si:H sample was deposited by plasma-enhanced chemical vapor deposition (PECVD) from silane in a conventional capacitively coupled reactor. The deposition conditions were a substrate temperature of 230 °C, a chamber pressure of 0.92 mbar, a flow rate of 40 sccm, and a frequency of 13.5 MHz. The sample thickness was 0.85 μm . Conductivity measurements were performed in the coplanar configuration, with a gap of 1 mm between two chromium electrodes.

In the moving photocarrier grating technique two coherent laser beams are brought to interfere on the surface of the sample. Thus, an intensity grating with spatial period $\Lambda = \lambda/[2 \sin(\delta/2)]$ is created, where δ is the angle between the two beams and λ is the laser wavelength. Since a small frequency shift Δf is introduced between the two beams, the resulting interference pattern moves with a velocity $v_{gr} = \Lambda \Delta f$. Due to their different mobilities, the photogenerated electron and hole distributions have a phase shift. This implies a grating-velocity-dependent short circuit current, which makes it possible to determine independently the photocarrier mobilities and the recombination lifetime (see Refs. 2 and 4).

The light intensity at the surface of the sample (coordinate x) has a spatial and temporal dependence:

$$I(x, t) = (I_1 + I_2) + 2\sqrt{I_1 I_2} \cos(kx - \omega_{gr} t), \quad (1)$$

where I_1 and I_2 are the intensities of the two beams, $k = 2\pi/\Lambda$, and $\omega_{gr} = 2\pi v_{gr}/\Lambda$. Our measurements were performed by using the $\lambda = 514$ nm line from an Ar laser and

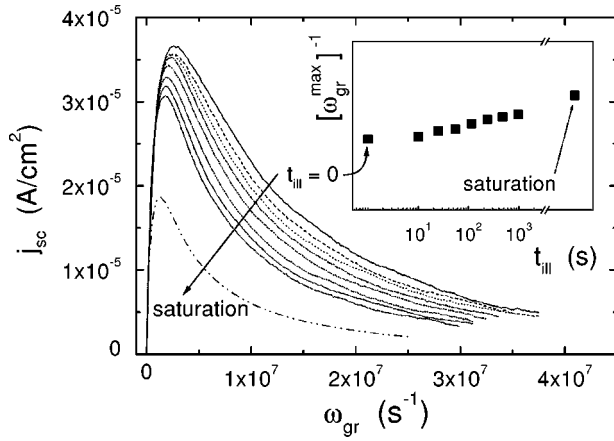


FIG. 1. Measured short circuit current density as a function of the grating angular frequency for different illumination times. Inset: the inverse of the angular frequency that gives a maximum short circuit current density, as a function of the illumination time. According to Ref. 2, in the lifetime regime $[\omega_{gr}^{max}]^{-1}$ is proportional to the recombination lifetime.

$\delta=31^\circ$, which gives $\Lambda=0.95 \mu\text{m}$. The intensities were $I_1=46 \text{ mW/cm}^2$ and $I_2=0.38 \text{ mW/cm}^2$. The light source for light soaking was the same Ar laser used for the MPG measurements, but we used an intensity approximately 10 times higher than the one used in the measurements. This ensures that the light-induced degradation during the measurement time can be neglected. We performed eight degradation steps from illumination time $t_{ill}=0$ to $t_{ill}=1000 \text{ min}$, and then a final degradation step with an intensity of $\approx 1000 \text{ mW/cm}^2$ up to saturation. Measurements and degradation were performed at room temperature.

III. RESULTS AND DISCUSSION

The effect of the light-induced degradation on the measured MPG curves can be seen in Fig. 1, where the short circuit current density j_{sc} is shown as a function of the grating angular frequency ω_{gr} . The short circuit current density decreases with the illumination time, and the maximum shifts towards lower grating angular frequencies. According to Haken, Hundhausen, and Ley,² in the lifetime regime, j_{sc} has a maximum for a grating angular frequency given by $\omega_{gr}^{max} \approx (\tau_R)^{-1}$. The inset in Fig. 1 shows $(\omega_{gr}^{max})^{-1}$ as a function of the illumination time. Since our measurements were performed in the lifetime regime, the increase of $(\omega_{gr}^{max})^{-1}$ shown in the inset of Fig. 1 would imply an increase of τ_R , which is unexpected under light-induced degradation. However, a more detailed analysis of the MPG method allows to clarify this apparent contradiction.

In the MPG technique the generation rate is given by

$$G(x,t) = G_0 + g \cos[kx - \omega_{gr}t], \quad (2)$$

where G_0 is related to (I_1+I_2) in Eq. (1) and g to $2\sqrt{I_1I_2}$. In the one-dimensional approximation the electron and hole densities $N(x,t)$ and $P(x,t)$ can be obtained from solution of the continuity equations

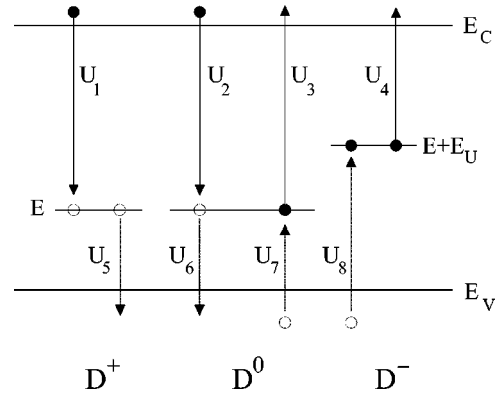


FIG. 2. Schematic representation of the electron (solid line) and hole (dotted line) flows for a single-dangling-bond level with correlation energy $E_U > 0$. Electrons are represented by solid circles and holes by open circles.

$$\frac{\partial N(x,t)}{\partial t} = \frac{1}{e} \frac{\partial j_n(x,t)}{\partial x} + G(x,t) - R(x,t), \quad (3)$$

$$\frac{\partial P(x,t)}{\partial t} = -\frac{1}{e} \frac{\partial j_p(x,t)}{\partial x} + G(x,t) - R(x,t), \quad (4)$$

where $j_n(x,t)$ and $j_p(x,t)$ are the electrons and holes current densities, respectively, and $R(x,t)$ is the recombination rate. In the case of amorphous materials, $N(x,t)$ and $P(x,t)$ include the concentrations of free and trapped photocarriers. In the treatment of HHL,² $R(x,t)$ is approximated by direct recombination between electrons and holes. However, it is known that for a sufficiently high defect density recombination proceeds mainly through dangling bond states. Especially for the sort of experiments that we have performed, where the dangling bond concentration increases as a function of illumination time, a more detailed treatment of recombination is needed.

A. Model to consider recombination

In order to simplify our treatment we will describe the corresponding equations for a single-dangling-bond level located at energy E_{DB} with a density N_{DB} per unit volume and represented by an amphotericlike state (correlation energy $E_U > 0$). Assuming that this defect can communicate with both the conduction band and the valence band, eight possible thermal processes will compete to set the occupation factor of this state in the absence of light. In Fig. 2 we sketch the eight possible thermal transitions. We make the usual assumption that dangling bonds can only capture mobile free carriers. Neither band-to-band transitions nor transitions between two dangling bonds are considered here because of their smaller probability. The number of thermal transitions per unit volume and unit time is named U_i and can be expressed as a function of the emission and capture parameters extending the Shockley-Read-Hall expressions to amphotericlike states:

$$\begin{aligned}
U_1 &= nN_D^+c_n^+, & U_2 &= nN_D^0c_n^0, & U_3 &= N_D^0e_n^0, \\
U_4 &= N_D^-e_n^-, & U_5 &= pN_D^0c_p^0, & U_6 &= pN_D^-c_p^-, \\
U_7 &= N_D^+e_p^+, & U_8 &= N_D^0e_p^0.
\end{aligned} \tag{5}$$

In these equations n and p are the densities of free electrons and holes, respectively; N_D^+ , N_D^0 , and N_D^- are the densities of positively charged, neutral, and negatively charged dangling bond centers, respectively; c_n^+ and c_n^0 are the capture coefficients (in $\text{cm}^3 \text{sec}^{-1}$) for electrons by D^+ and D^0 states, respectively; c_p^0 and c_p^- are the capture coefficients for holes by D^0 and D^- states, respectively; e_n^0 and e_n^- are the emission coefficients for electrons from D^0 and D^- states, respectively; and e_p^+ and e_p^0 are the emission coefficients for holes from D^+ and D^0 states, respectively. The capture coefficients, c_n^+ , c_n^0 , c_p^0 , and c_p^- are given by the well-known relations $c_n^+ = v_{th}\sigma_n^+$, $c_n^0 = v_{th}\sigma_n^0$, $c_p^0 = v_{th}\sigma_p^0$, and $c_p^- = v_{th}\sigma_p^-$, where σ_n^+ , σ_n^0 , σ_p^0 , and σ_p^- are the corresponding capture cross sections and v_{th} is the free carrier thermal velocity. Under thermodynamic equilibrium conditions the principle of detailed balance must be satisfied; thus, $U_1 = U_3$, $U_2 = U_4$, $U_5 = U_6$, and $U_7 = U_8$. Taking into account Eq. (5) this leads to the following equalities:

$$\begin{aligned}
e_n^0 &= (n)_0(N_D^+)_0c_n^+/(N_D^0)_0, \\
e_n^- &= (n)_0(N_D^0)_0c_n^0/(N_D^-)_0, \\
e_p^0 &= (p)_0(N_D^-)_0c_p^-/(N_D^0)_0, \\
e_p^+ &= (p)_0(N_D^0)_0c_p^0/(N_D^+)_0,
\end{aligned} \tag{6}$$

where the subscript “0” stands for thermodynamic equilibrium. Under nonequilibrium we make the usual assumption that the emission and capture rates remain unaltered with respect to equilibrium conditions. The recombination rate is given by

$$R(x,t) = [U_1(x,t) - U_3(x,t)] + [U_2(x,t) - U_4(x,t)] \tag{7}$$

or, equivalently,

$$R(x,t) = [U_5(x,t) - U_7(x,t)] + [U_6(x,t) - U_8(x,t)]. \tag{8}$$

Replacing in Eq. (7) the U_i values from Eq. (5) we get

$$R(x,t) = [nN_D^+c_n^+ - N_D^0e_n^0] + [nN_D^0c_n^0 - N_D^-e_n^-] \tag{9}$$

or, from Eq. (8),

$$R(x,t) = [pN_D^0c_p^0 - N_D^+e_p^+] + [pN_D^-c_p^- - N_D^0e_p^0]. \tag{10}$$

The rate equations for the dangling bond concentrations are

$$\frac{\partial N_D^+}{\partial t} = U_3 + U_5 - U_1 - U_7, \tag{11}$$

$$\frac{\partial N_D^-}{\partial t} = U_2 + U_8 - U_4 - U_6,$$

$$\frac{\partial N_D^0}{\partial t} = U_1 + U_4 + U_6 + U_7 - U_2 - U_3 - U_5 - U_8.$$

In the case of uniform illumination [i.e., $G(x,t) = G_0$], a steady state is reached if the rates in Eqs. (3), (4), and (11) are equal to zero. The solution of the resulting system of algebraic equations gives the steady-state values of N , P , N_D^+ , N_D^0 , and N_D^- , which will be distinguished by the subscript *hom*. Thus, N_{hom} is the steady-state concentration of free plus trapped electrons under homogeneous illumination. On the other hand, when the generation rate has a spatial and temporal dependence as in Eq. (2), the solution of the system of differential equations (3), (4), and (11) allows us to obtain $N(x,t)$, $P(x,t)$, $N_D^+(x,t)$, $N_D^0(x,t)$, and $N_D^-(x,t)$. We solve the system of differential equations as in Ref. 2, assuming that the relevant physical parameters vary sinusoidally as $G(x,t)$ does and allowing for proper phase shifts. The presence of a distribution of charge within the material leads to an internal electric field $E(x,t)$, given by solution of Poisson's equation

$$\frac{\partial E(x,t)}{\partial x} = \frac{e}{\epsilon\epsilon_0} \{P(x,t) + N_D^+(x,t) - N(x,t) - N_D^-(x,t)\}. \tag{12}$$

If this electric field is in phase with $N(x,t)$ and $P(x,t)$, a short circuit current arises, given by the spatial average of the drift current over one period:

$$j_{sc} = \frac{1}{\Lambda} \int [e\mu_n N(x,t) + e\mu_p P(x,t)] E(x,t) dx. \tag{13}$$

By using an approximate expression for the recombination, the authors in Ref. 2 could find an analytical solution of Eq. (13). However, when the expression given in Eq. (9) [or Eq. (10)] is used for the recombination, the equations are no longer analytically solvable and only a numerical solution is possible. This means that the experimental curves cannot be fitted but only simulated with reasonable values for the parameters.

B. Choice of the parameters

The mobility gap was taken as $E_\mu = 1.8$ eV. The densities of states at the band edges were assumed to be equal, $N(E_C) = N(E_V) = 5 \times 10^{21} \text{ cm}^{-3} \text{ eV}^{-1}$. The dangling bond level was placed at an energy in the middle of the mobility gap, $E_{DB} = 0.9$ eV, and the correlation energy was assumed to be $E_U = 0.2$ eV. The free carrier thermal velocity was taken as $v_{th} = 10^7$ cm/s both for electrons and holes. The electron and hole capture cross sections of the neutral dangling bonds were taken to be equal, $\sigma_n^0 = \sigma_p^0 = 3.0 \times 10^{-16} \text{ cm}^2$. Due to the Coulombic attraction, the capture cross sections of the charged defects were taken as 10 times larger, $\sigma_n^+ = \sigma_p^- = 3.0 \times 10^{-15} \text{ cm}^2$. These values are within the usual experimental range.^{7,8} The drift mobilities for elec-

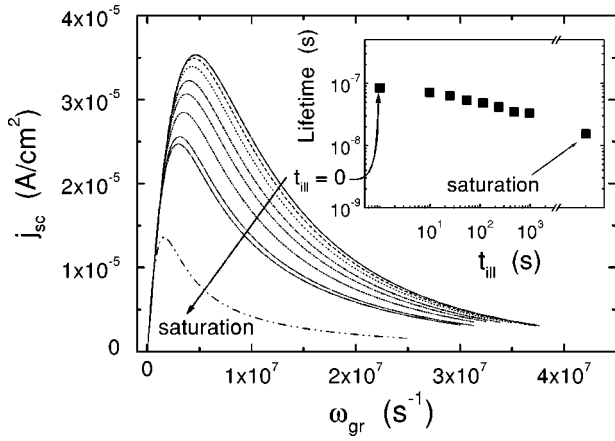


FIG. 3. Simulated short circuit current density as a function of the grating angular frequency for different illumination times. Inset: the simulated electron lifetime, obtained as $\tau_{sim} = N_{hom}/G_0$.

trons and holes were taken from Ref. 2, $\mu_N = 0.077 \text{ cm}^2 \text{ V}^{-1} \text{ s}^{-1}$ and $\mu_P = 0.005 \text{ cm}^2 \text{ V}^{-1} \text{ s}^{-1}$, and are compatible with independent measurements of the same material.⁹ The carrier mobilities in extended states were taken as 10 times larger than the corresponding drift mobilities. These values are quite low compared to the most accepted values $\mu_N^0 = 10 \text{ cm}^2 \text{ V}^{-1} \text{ s}^{-1}$ and $\mu_P^0 = 1 \text{ cm}^2 \text{ V}^{-1} \text{ s}^{-1}$ (Ref. 10), but provide the best agreement to the initial state curve (the one for illumination time $t_{ill} = 0$). The defect density in the initial state was measured by photothermal deflection spectroscopy (PDS), obtaining $N_{DB} = 5 \times 10^{16} \text{ cm}^{-3}$. The defect density is the single parameter that evolves as a function of t_{ill} . To estimate this evolution we have taken into account the decay of the photoconductivity:

$$\sigma_{ph}(t_{ill}) = qG_0\mu_N^0\tau_N^0(t_{ill}),$$

where q is the electron charge, μ_N^0 is the free electron mobility, and $\tau_N^0(t_{ill})$ is the time-dependent free electron lifetime, given by

$$\tau_N^0(t_{ill}) = 1/[v_{th}\sigma_n^0 N_D^0(t_{ill}) + v_{th}\sigma_n^+ N_D^+(t_{ill})] \propto 1/[N_{DB}(t_{ill})].$$

We have considered that μ_N^0 and the capture cross sections do not change with t_{ill} , thus obtaining $N_{DB}(t_{ill})$ from $[\sigma_{ph}(t_{ill})]^{-1}$.

C. Simulations

In Fig. 3 we present the simulated short circuit current densities as a function of the grating angular frequency for the same illumination times of Fig. 1. All the parameters remain fixed except for the defect density, which was estimated as mentioned before. As can be seen, the simulations reproduce the general trend of the measured curves in Fig. 1. The short circuit current density tends to decrease and the maximum shifts towards lower grating angular frequencies. There is a difference in the actual position of the maximum, and the effect of degradation is larger in the simulations than in the measurements, but taking into account that the parameters are not further adjusted for each illumination time the

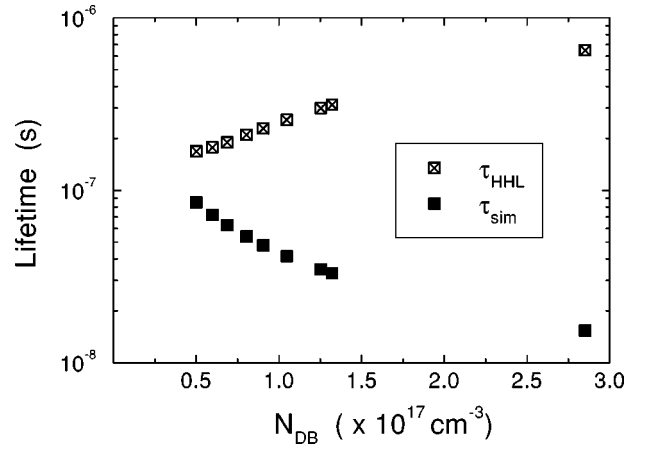


FIG. 4. Recombination lifetime obtained from a fit of the simulated curves of Fig. 3 with the HHL formula (τ_{HHL} , crossed squares) and from the simulations as N_{hom}/G_0 (τ_{sim} , solid squares).

agreement is acceptable. As a result of the simulations the steady-state electron concentration under homogeneous illumination, N_{hom} , is also obtained. The simulated recombination lifetime, calculated as $\tau_{sim} = N_{hom}/G_0$, is shown in the inset of Fig. 3 as a function of t_{ill} . Figure 4 shows the dependence of the recombination lifetime on the defect density. A fit of the simulated MPG curves of Fig. 3 with the formula deduced in Ref. 2 gives the recombination lifetime shown as crossed squares (τ_{HHL}). This ‘‘apparent’’ lifetime increases with N_{DB} , just like τ_R obtained from the measured curves as $[\omega_{gr}^{max}]^{-1}$ (shown in the inset of Fig. 1). However, the recombination lifetime obtained from the simulations as $\tau_{sim} = N_{hom}/G_0$ decreases with N_{DB} , as expected due to the increase in the density of recombination centers. Note that for lower defect densities ($t_{ill} \rightarrow 0$), τ_{HHL} and τ_{sim} tend to agree, meaning that the HHL formula is applicable for α -Si:H of low defect density. The HHL treatment has the advantage of being analytical, meaning that a close expression for j_{sc} as a function of ω_{gr} is obtained. A fit of the measured j_{sc} curves with the HHL expression allows us to obtain initial estimates for the drift mobilities and the recombination lifetime, which can be further refined by using the complete treatment that we have developed here. Thus, the MPG method can be confidently used to determine the drift mobilities and recombination lifetime of semiconductors.

IV. CONCLUSION

In this work we have addressed some inconsistencies arising from the application of the MPG method to samples with a high defect density. The approximate treatment of Haken, Hundhausen, and Ley² leads to an apparent increase of the recombination lifetime upon light-induced degradation, which is contradictory to the expected increase of the defect density. This approximate treatment has been refined by explicitly including recombination through dangling bond states. The extended treatment presented here allows us to reproduce the evolution of the measured curves by changing the defect density only. Moreover, the lifetime obtained from

the solution of the transport equations decreases with the illumination time, as expected. The lifetime values obtained from the extended and approximate treatments tend to agree for samples with a low defect density, indicating that the second method can be used to provide an initial estimate for the parameters.

ACKNOWLEDGMENTS

J.A.S. gratefully acknowledges support from the Alexander von Humboldt Foundation and the Fundacion Antorchas.

-
- ¹U. Haken, M. Hundhausen, and L. Ley, *Appl. Phys. Lett.* **63**, 3066 (1993).
²U. Haken, M. Hundhausen, and L. Ley, *Phys. Rev. B* **51**, 10 579 (1995).
³J. Schmidt, M. Hundhausen, and L. Ley, *Phys. Rev. B* **62**, 13 010 (2000).
⁴M. Hundhausen, *J. Non-Cryst. Solids* **198-200**, 146 (1996).
⁵G. Priebe, B. Pietzak, and R. Konenkamp, *Appl. Phys. Lett.* **71**, 2160 (1997).
⁶D.L. Staebler and C.R. Wronski, *Appl. Phys. Lett.* **31**, 292 (1977).
⁷A. Mittiga, P. Fiorini, M. Sebastiani, S. Korepanov, and F. Evangelisti, in *Proceedings of the 21th IEEE Photovoltaic Specialists Conference*, edited by Dennis Flood (IEEE, New York, 1990), p. 1465.
⁸S. Lee, M. Günes, C.R. Wronski, N. Maley, and M. Bennett, *Appl. Phys. Lett.* **59**, 1578 (1991).
⁹K. Hattori, H. Okamoto, and Y. Hamakawa, *Phys. Rev. B* **45**, 1126 (1992).
¹⁰R. A. Street, *Hydrogenated Amorphous Silicon* (Cambridge University, Cambridge, England, 1991), p. 237.